2020 IEEE 9th Joint International Information Technology and Artificial Intelligence Conference (ITAIC) | 978-1-7281-5244-8/20/$31.00 ©2020 IEEE | DOI: 10.1109/ITAIC49862.2020.9338865

An Analytical Solution to Inverse Kinematics of Seven Degree-of-freedom Redundant Manipulator

Jiaxin Guo[1] , Yihan Xu[1] , Cong Huang[1] , Xufeng Zhu[1] , Chuqi Shao[1]
1. Beijing Aerospace Automatic Control Institute, China Academy of Launch Vehicle Technology, Beijing, China
791132510@qq.com, 2250592476@qq.com, 1161472812@qq.com, zhuxufeng@126.com, 17888835860@163.com
Corresponding Author: Jiaxin Guo Email: 791132510@qq.com

***Abstract*—This paper proposes an analytic inverse kinematics computation method for redundant manipulator with S-R-S configuration. Forward kinematics model is built based on traditional D-H modeling approach. The redundancy is decoupled through designing the virtual arm angle parameters and the relationship between arm angle and joint angle is detailed. A complete analytic inverse kinematics equation in position space is obtained, which eliminates the acquisition of joint speed and Jacobian matrix. And the optimal strategy to obtain inverse kinematics under joint limits is designed. The method is verified using robotics toolbox and simulation is made on the ROS platform.**

Keywords—inverse kinematics; arm angle; redundant manipulator;ROS simulation

I. INTRODUCTION

The robot is an effective tool to replace humans in repetitive and high-risk operation. Traditional robot with six degrees of freedom can only reach the position in the operating space with limited pose. However, the redundant manipulator with seven degrees of freedom can finish more tasks in the operating space due to redundancy design. In the aerospace field, maintenance and repair of the international space station [1] and on-orbit maintenance of the satellite [2] are completed via platform with seven degrees of freedom. Inverse kinematics is to establish the mapping relationship between the target pose and the robot arm joint angle which is the basis for exerting the movement ability of the manipulator and provides the basis for control and planning.

Because of redundancy, the inverse kinematics of redundant manipulator is a one-to-many and highly nonlinear process and it's difficult to build the analytic mapping relation directly. Solving inverse kinematics by neural network is conducted in [4] and [5]. The neural network is of very high fitting precision, so the final solution can be used for grasping of desktop objects and man-machine interaction based on lots of testing and learning in the early stage. However, there is a big gap between learned model and accurate applications. And it's hard to use the model for real-time control.

The null space of Jacobian matrix can also be used for finding a valid solution near current configuration. The motion of end actuator in the Cartesian space is mapped to the joint space through Jacobian matrix and different constraints can be met when searching in the null space, such as optimal moveability [6], optimal joint torque [7], obstacle avoidance [8, 9] and singularity avoidance [10, 11]. However, it's also hard to be conducted for accurate applications (such as handling and assembly). Moreover, it's difficult to quantify the angle range constraints of each joint to avoid reaching joint limits.

Based on the kinematic solving method of robot arm with six degrees of freedom, all joint angles are fixed successively to obtain the multiple solutions for the target pose, the minimum norm method is designed [12, 13] and the norm can be chosen to meet the constraints of target pose. As for the above method, the inverse kinematics solution strategy of robot arm with six degrees of freedom can be fully used to obtain the kinematics formula in analytic form. The disadvantage of such strategy is always selecting a joint angle for fixation during movement and failing to exert the motion ability of manipulator.

The inverse kinematics solution strategy based on the arm angle strategy is proposed, the arm angle is used to accomplish the decoupling of robot arm with seven degrees of freedom and the joint angle range constraint is introduced by arm angle optimization process[14,15]. The analytic inverse kinematics equation completely based on position is obtained which is convenient for realizing high-precision motion control of the end effector [16] and such method is further expanded to the inverse kinematics solving process of space robot. The strategy based on arm angle is also used for kinematic solution of the robot arm with wrist and elbow offset configuration[17,18]. The inverse kinematics solution strategy based on arm angle strategy is systematically analyzed and stated in [19] and the joint limit avoidance and singularity avoidance is optimized altogether. Although the solution strategy is widely developed and applied, the analysis in previous literature is neither complete nor sufficient.

According to the requirements against new space applications and space explorations, this paper puts forward the complete analytic inverse kinematics for the robot arm with S-R-S configuration: Firstly, the mapping relation between the joint angle and end actuator pose is

deduce, and then the arm angle constraint is introduced, the range of joint rotation is used as optimizing constrait. And the mapping relation between the arm angle and the joint angle is systematically stated. Finally, the robotics toolbox and ROS platform are used for verification && simulation of the algorithm proposed.

II. MODELING AND ANYLYSIS

This chapter builds the kinematics model of the 7-DOF manipulator, introduces the concept of arm angle constraint, decouples the redundancy, and then derives the optimal inverse kinematics solution strategy when the joint range is limited.

A. Modeling of Manipulator

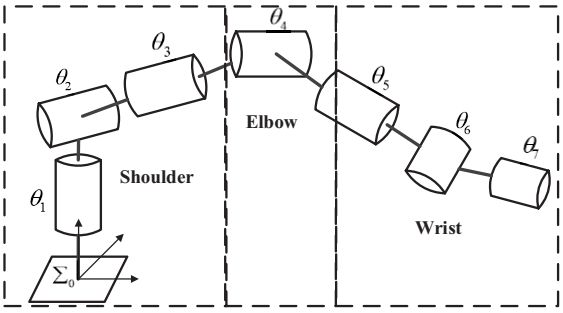

Fig.1 Manipulator with S-R-S Configuration

The S-R-S configuration manipulator is selected as the analysis object, which is the most common configuration used in space and service robots. The manipulator contains a total of 7 joints from the base to the end effector, of which the first three joints are perpendicular to each other and intersect at one point, forming a homogenous association pattern with the Sphere, called the shoulder joint; the joint axes of the last three joints are perpendicular to each other and intersect at one point, forming a homogenous association pattern with the Sphere, called the wrist joint; the middle joint is a rotate joint called the elbow joint. The shoulder joint, elbow joint and wrist joint cascade to form an S-R-S configuration, as shown in Figure 1.

Based on the D-H (Denavit-Hartenberg) rule, the forward kinematics of manipulator is build according to the parameters listed in Table I.

Table I D-H Parameter

i	θ_i	α_i	d_i	a_i
1	θ_1	$-\pi/2$	d_{bs}	0
2	θ_2	$\pi/2$	0	0
3	θ_3	$-\pi/2$	d_{se}	0
4	θ_4	$\pi/2$	0	0
5	θ_5	$-\pi/2$	d_{ew}	0
6	θ_6	$\pi/2$	0	0
7	θ_7	0	d_{wt}	0

B. Decoupling of Redundancy

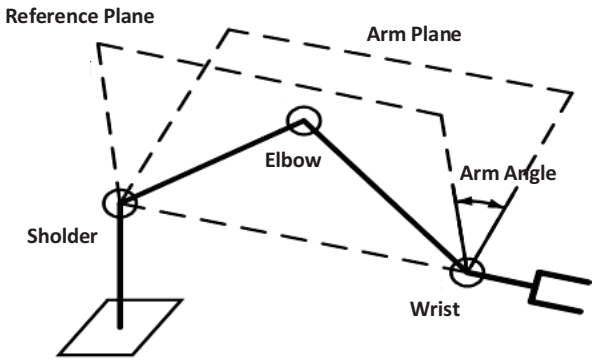

Fig.2 Arm Angle for Decoupling

The manipulator has 7 rotating joint relative to pose of the end effector in Cartesian space, and the mapping between joint space and Cartesian space is redundant and nonlinear. In order to obtain the inverse kinematics in analytical form, it is necessary to parameterize the redundancy using additional constraints. In [12], the one joint axis is selected from the 7 joint axes for fixation, and then the solution is solved in the manner of 6 joint degrees of freedom. In [20], the self-motion of manipulators is used for redundancy decoupling, but this kind of decoupling method cannot be extended to manipulators of general configuration.

The main idea of the redundant decoupling method based on arm angle is to use the angle between the plane formed by the elbow, shoulder and wrist (arm plane) and the reference plane to form an extra degree of freedom. The extended freedom is introduced as constraints to form the inverse kinematics in an analytical way. However, the existing analysis in literature is not sufficient. This article aims to provide a detailed induction process and analysis.

C. Froward Kinematics

For the redundant manipulator in the S-R-S configuration, the reference plane is defined as the plane formed by the elbow, shoulder, and wrist when θ_3 is at 0. In an ideal situation, the pose of end effector remain unchanged as arm angle changes from 0 to 360° along the reference plane. And different inverse kinematics solutions can be obtained with different arm angle constraint.

The pose of the end effector is represented by the position vector $x_7^0 \in \Re^3$ and the roatation matrix $R_7^0 \in SO(3)$ relative to the base coordinate system $\sum_0$.

The forward kinematics can be obtained using the relationship of the end effector pose under the given joint axis coordinates:

$$x_7^0 = l_{bs}^0 + R_3^0 \left(l_{se}^3 + R_4^3 \left(l_{ew}^4 + R_7^4 l_{wt}^7 \right) \right) \qquad (1)$$

$$R_7^0 = R_3^0 R_4^3 R_7^4 \tag{2}$$

The superscript represents the reference coordinate system, and the subscript is the relative coordinate system. R_j^i represents the rotation of the coordinate system $\sum_j$ relative to $\sum_i$. l_{bs}^0, l_{se}^3, l_{ew}^4 and l_{wt}^7 are constant vectors:

$$l_{bs}^0 = [0 \quad 0 \quad d_{bs}]^T$$

$$l_{se}^3 = [0 \quad -d_{se} \quad 0]^T$$

$$l_{ew}^4 = [0 \quad 0 \quad d_{ew}]^T$$

$$l_{wt}^7 = [0 \quad 0 \quad d_{wt}]^T$$

In the case of D-H modeling, the posture of the coordinate system $\sum_i$ relative to $\sum_{i-1}$. is:

$$R_i^{i-1} = \begin{bmatrix} \cos\theta_i & -\sin\theta_i \cos\alpha_i & \sin\theta_i \sin\alpha_i \\ \sin\theta_i & \cos\theta_i \cos\alpha_i & -\cos\theta_i \sin\alpha_i \\ 0 & \sin\alpha_i & \cos\alpha_i \end{bmatrix} \tag{3}$$

For the redundant manipulator with S-R-S configuration, when the arm angle reference plane is determined, the self-motion of the manipulator is defined as the arm plane rotating along the straight line formed by shoulder and wrist position. First, it is necessary to obtain the spatial representation of the straight line to pave the way for the introduction of arm angle as well as kinematics optimization.

Use $x_{sw}^0 \in \Re^3$ to represent the vector from the shoulder joint to the wrist joint, we can obtain:

$$\begin{aligned} x_{sw}^0 &= x_7^0 - l_{bs}^0 - R_7^0 l_{wt}^7 \\ &= R_3^0 \left(l_{se}^3 + R_4^3 l_{ew}^4 \right) \end{aligned} \tag{4}$$

When the pose of the end effector is fixed, since the elements in equation (4) remain unchanged, x_{sw}^0 remain unchanged. Therefore, the manipulator can keep the position of the end effector unchanged during the self-motion process. However, the posture of the wrist joint relative to the base coordinate system changes during the self-motion process. Use the symbol φ to represent arm angle, and from Rodriguez's rotation formula, the rotation of the wrist caused by arm angle is:

$$R_\varphi^0 = I_3 + \sin\varphi [u_{sw}^0 \times] + (1 - \cos\varphi)[u_{sw}^0 \times]^2 \tag{5}$$

where $I_3 \in \Re^{3\times3}$ is the unit matrix, u_{sw}^0 is the normalized unit length vector of x_{sw}^0 , and $[u_{sw}^0 \times]$ is the skew symmetric matrix of u_{sw}^0 . Therefore, the posture of the wrist joint relative to the base coordinate system is expressed as:

$$R_4^0 = R_\varphi^0 R_4^{0O} \tag{6}$$

where R_4^{0O} represents the posture matrix of the wrist joint when the arm angle plane coincides with the reference plane ($\varphi = 0$).

When x_{sw}^0 remains unchanged during the self-motion process, we can get from equation (4):

$$\left\| x_{sw}^0 \right\| = \left\| \left(l_{se}^3 + R_4^3 l_{ew}^4 \right) \right\| \tag{7}$$

l_{se}^3 and l_{ew}^4 are fixed vectors, which is obtained from the fact that the angle of the elbow joint does not change. Therefore, equation (6) can be simplified as:

$$R_3^0 = R_\varphi^0 R_3^{0O} \tag{8}$$

Bringing them into equations (1) and (2), the forward kinematics after the introduction of self-motion is:

$$x_7^0 = l_{bs}^0 + R_\varphi^0 R_3^{0O} \left(l_{se}^3 + R_4^3 \left(l_{ew}^4 + R_7^4 l_{wt}^7 \right) \right) \tag{9}$$

$$R_7^0 = R_\varphi^0 R_3^{0O} R_4^3 R_7^4 \tag{10}$$

D. Inverse Kinematics

Assuming that the desired end effector position and posture are $\tilde{x}_7^0$ and $\tilde{R}_7^0$ respectively, based on equations (9) and (10), the steps to calculate joint angles that satisfy the pose constraints are as follows:

First, the calculation formula for the elbow joint angle is:

$$\cos\theta_4 = \frac{\left\| x_{sw}^0 \right\|^2 - d_{se}^2 - d_{ew}^2}{2 d_{se} d_{ew}} \tag{11}$$

And x_{sw}^0 is calculated using following formula:

$$x_{sw}^0 = \tilde{x}_7^0 - l_{bs}^0 - \tilde{R}_7^0 l_{wt}^7 \tag{12}$$

Then, there are three joint axes intersecting at shoulder. Their joint angles are related to the value of arm angle. and first calculate the angle of the shoulder joint when the When arm angle is 0($\theta_3 = 0$), we can obtain:

$$x_{sw}^0 = R_1^{0O} R_2^{1O} R_3^2 \Big|_{\theta_3=0} \left(l_{se}^3 + R_4^3 l_{ew}^4 \right) \tag{13}$$

where θ_4 is calculated by formula (11). At this time, the unknown variables are θ_1^O and θ_2^O . As x_{sw}^0 is fixed, when φ is given, substituting (5) into (8) to obtain:

$$R_3^0 = A_s \sin\varphi + B_s \cos\varphi + C_s \tag{14}$$

where, A_s , B_s and C_s are constant matrices:

$$A_s = [u_{sw}^0 \times] R_3^{0O}$$

$$B_s = -[u_{sw}^0 \times]^2 R_3^{0O}$$

$$C_s = [u_{sw}^0 \left(u_{sw}^0\right)^T] R_3^{0O}$$

The rotation matrix R_3^0 is derived from forward kinematics (where * has no effect on the solution):

$$R_3^0 = \begin{bmatrix} * & -\cos\theta_1 \sin\theta_2 & * \\ * & -\sin\theta_1 \sin\theta_2 & * \\ -\sin\theta_2 \cos\theta_3 & -\cos\theta_2 & \sin\theta_2 \sin\theta_3 \end{bmatrix}$$

Thus we can obtain the relationship between arm angle and the angle of joint around shoulder:

$$\tan\theta_1 = \frac{-a_{s22}\sin\varphi - b_{s22}\cos\varphi - c_{s22}}{-a_{s12}\sin\varphi - b_{s12}\cos\varphi - c_{s12}} \tag{15}$$

$$\cos\theta_2 = -a_{s32}\sin\varphi - b_{s32}\cos\varphi - c_{s32} \tag{16}$$

$$\tan\theta_3 = \frac{a_{s33}\sin\varphi + b_{s33}\cos\varphi + c_{s33}}{-a_{s31}\sin\varphi - b_{s31}\cos\varphi - c_{s31}} \tag{17}$$

In the formula, a_{sij} , b_{sij} and c_{sij} correspond to the element (i, j) in A_s , B_s and C_s respectively. Given the arm angle, three joint angles around shoulder can be obtained.

Finally, after obtaining the angles around shoulder and elbow, we can calculate the rotation angles of the three axes around wrist joint. Substituting (5) into (10) to obtain:

$$R_7^4 = A_w \sin\varphi + B_w \cos\varphi + C_w \tag{18}$$

where, A_s , B_s and C_s are constant matrices:

$$A_w = \left(R_4^3\right)^T \left(A_s\right)^T \tilde{R}_7^0$$

$$B_w = \left(R_4^3\right)^T \left(B_s\right)^T \tilde{R}_7^0$$

$$A_w = \left(R_4^3\right)^T \left(C_s\right)^T \tilde{R}_7^0$$

From forward kinematics, the algebraic form of the rotational matrix:

$$R_7^4 = \begin{bmatrix} * & * & \cos\theta_5 \sin\theta_6 \\ * & * & \sin\theta_5 \sin\theta_6 \\ -\sin\theta_6 \cos\theta_7 & \sin\theta_6 \sin\theta_7 & \cos\theta_6 \end{bmatrix}$$

Thus, the relationship between the arm angle and the three joint angles around wrist expressed as:

$$\tan\theta_5 = \frac{a_{w23}\sin\varphi + b_{w23}\cos\varphi + c_{w23}}{a_{w13}\sin\varphi + b_{w13}\cos\varphi + c_{w13}} \tag{19}$$

$$\cos\theta_6 = a_{w33}\sin\varphi + b_{w33}\cos\varphi + c_{w33} \tag{20}$$

$$\tan\theta_7 = \frac{a_{w32}\sin\varphi + b_{w32}\cos\varphi + c_{w32}}{-a_{w31}\sin\varphi - b_{w31}\cos\varphi - c_{w31}} \tag{21}$$

Given the arm angle, the three joint angles around wrist can be calculated through above equation.

E. Singularity

In the absence of singularity, the analytical inverse kinematics calculation scheme can be directly obtained relying on the formula above. However, in the case of singular joints, it is necessary to design a special way to avoid uncertain motion of the manipulator.

For the manipulator with S-R-S configuration, the singular situations involved in the inverse kinematics include shoulder singularity, elbow singularity and wrist singularity [21]. Among them, the wrist singularity will not cause sudden changes in joint movement. The singularity of the elbow occurs when the trajectory point exceeds the reaching range of manipulator, in which the elbow joint is fully extended. Such situations can be directly obtained by analyzing the reachability of the target pose.

In shoulder singularity, the method proposed in this paper may cause uncertainty of joint motion. If the wrist joint lies on the extension line of the joint axis 1, θ_1 and θ_7 have the same effect on the posture of the end effector. In the previous literature, θ_1 is forced to equal φ to decouple θ_1 and θ_7 .

This paper adopts a different strategy. When the next target pose point is detected as leading to shoulder singularity, θ_1 keeps unchanged and θ_7 is computed in decoupled manner. The advantage of this strategy is that it can minimize the rotation of θ_1 and avoid jumping movement of the manipulator body.

III. ARM ANGLE SELECTION

Ideally, when the arm angle changes from 0 to 2π, numerous inverse kinematics solutions can be obtained. In the process of robot arm design, each joint axis of the redundant manipulator with S-R-S configuration is of a limited rotation range other than ideal 2π range due to physical constraints such as movement reachability and self-collision. Thus when target pose is set, it's necessary to select the optional arm angle to meet those constraints and avoid reaching the range limit.

According to (15)-(17) and (19)-(20), the joint angle calculation of spherical joint (shoulder joint and wrist joint) can be classified as:

$$\tan\theta_i = \frac{a_n \sin\varphi + b_n \cos\varphi + c_n}{a_d \sin\varphi + b_d \cos\varphi + c_d} \tag{22}$$

$$\cos\theta_i = a\sin\varphi + b\cos\varphi + c \tag{23}$$

These two formulas represent two different features when mapping between the arm angle and joint axis--tangent type and cosine type, respectively.

A. Tangent Type

The relationship between joint angle and arm angle can be expressed with the following formula:

$$\tan\theta_i = \frac{f_n(\varphi)}{f_d(\varphi)} \tag{24}$$

wherein, $f_n(\varphi)$ and $f_d(\varphi)$ represent:

$$f_n(\varphi) = a_n \sin\varphi + b_n \cos\varphi + c_n$$
$$f_d(\varphi) = a_d \sin\varphi + b_d \cos\varphi + c_d$$

Take the differentiation of (24) with respect to φ, following result is obtained:

$$\frac{d\theta_i}{d\varphi} = \frac{a_t \sin\varphi + b_t \cos\varphi + c_t}{f_d^2(\varphi) + f_n^2(\varphi)} \tag{25}$$

wherein, a_t, b_t and c_t are given by the following equation:

$$a_t = b_d c_n - b_n c_d$$
$$b_t = c_d a_n - c_n a_d$$
$$c_t = b_d a_n - b_n a_d$$

When the following formula holds, the relation curve between arm angle and joint angle has a limit point:

$$a_t^2 + b_t^2 - c_t^2 > 0 \tag{26}$$

And θ_i obtained limit value (maximum or minimum) at following two arm angles:

$$\varphi_0^- = 2\tan^{-1}\frac{a_t - \sqrt{a_t^2 + b_t^2 - c_t^2}}{b_t - c_t} \tag{27}$$

$$\varphi_0^+ = 2\tan^{-1}\frac{a_t + \sqrt{a_t^2 + b_t^2 - c_t^2}}{b_t - c_t} \tag{28}$$

After the analysis of second order derivative, the θ_i take extreme value at φ_0^- or φ_0^+. And the extreme value is global maximum or global minimum. It should be noted that the magnitude of φ_0^- and φ_0^+ cannot be as the signs of a_t, b_t and c_t cannot be confirmed in advance.

When the following formula holds, the relationship between arm angle and joint angle is a monotone curve:

$$a_t^2 + b_t^2 - c_t^2 < 0 \tag{29}$$

$\theta_i(\varphi)$ is a monotone curve and θ_i takes the extreme at the boundary of φ.

In case of $a_t^2 + b_t^2 - c_t^2 = 0$, θ_i has single extreme value when:

$$\varphi_0 = 2\tan^{-1}\frac{a_t}{b_t - c_t} \tag{30}$$

In this case, the numerator and denominator in formula (24) are all 0 which falls into a singular state. And the value of θ_i cannot be determined at this point.

To know the relationship between the arm angle and θ_i under the singular situation. Following result can be obtained according to formula (24) after calculating the relationship between θ_i and φ under small increment δ:

$$\tan\theta_i = \frac{\frac{\sin\delta}{c_t}\left((1+\cos\delta)(a_t b_n - b_t a_n) + c_t c_n \sin\delta\right)}{\frac{\sin\delta}{c_t}\left((1+\cos\delta)(a_t b_d - b_t a_d) + c_t c_d \sin\delta\right)} \tag{31}$$

When δ reaches to zero from the left side and right side, respectively, the following result can be obtained:

$$\lim_{\delta\to-0}\tan\theta_i=\frac{\frac{-1}{c_t}\left(a_tb_n-b_ta_n\right)}{\frac{-1}{c_t}\left(a_tb_d-b_ta_d\right)} \tag{32}$$

$$\lim_{\delta\to+0}\tan\theta_i=\frac{\frac{1}{c_t}\left(a_tb_n-b_ta_n\right)}{\frac{1}{c_t}\left(a_tb_d-b_ta_d\right)} \tag{33}$$

Under such state, when the numerator and denominator in the right formula aren't zero, the difference between θ_i values with left limit and right limit reaches to π. When the numerator in formula (32) or (33) is zero, the difference between θ_i values with left limit and right limit reaches to 2π.

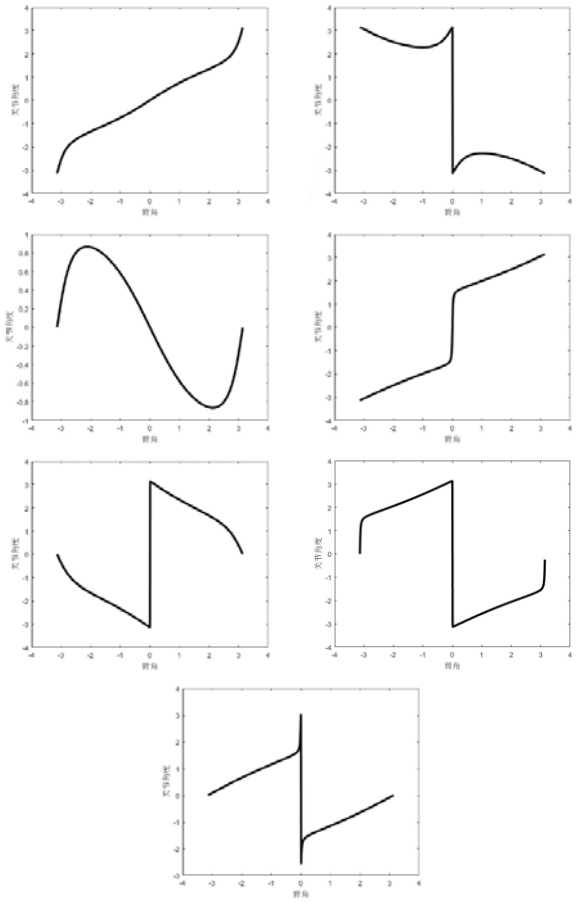

Fig.3 Relation Curve of Tangent Type

In previous literatures, only four possible relation curves between θ_i and φ in tangent type is listed and 7 possible relation curves are discovered in total, as shown in Fig 3.

B. Cosine Type

According to formula (23), taking the derivation on both sides with respect to φ, the following result is obtained:

$$\frac{d\theta_i}{d\varphi}=-\frac{1}{\sin\theta_i}\left(a\cos\varphi-b\sin\varphi\right) \tag{34}$$

If $\sin\theta_i$ isn't zero, there are two extreme points:

$$\varphi_0^-=2\tan^{-1}\frac{-b-\sqrt{a^2+b^2}}{a} \tag{35}$$

$$\varphi_0^+=2\tan^{-1}\frac{-b+\sqrt{a^2+b^2}}{a} \tag{36}$$

wherein, θ_i is global maximum or minimum at two extreme points. And when $\sin\theta_i$ is zero, following result can be obtained:

$$a^2+b^2-\left(c-1\right)^2=0 \tag{37}$$

or

$$a^2+b^2-\left(c+1\right)^2=0 \tag{38}$$

When formula (37) is satisfied, the arm angle is:

$$\varphi_0=2\tan^{-1}\frac{a}{b-\left(c-1\right)} \tag{39}$$

$\theta_i=0$ in this situation. The gradient at the arm angle cannot be determined. After limit value analysis under the small change δ, it can be known that the left limit and right limit are:

$$\lim_{\delta\to-0}\frac{d\theta_i}{d\varphi}=-\sqrt{1-c} \tag{40}$$

$$\lim_{\delta\to-0}\frac{d\theta_i}{d\varphi}=\sqrt{1-c} \tag{41}$$

Similarly, when the condition (38) is met, the arm angle is:

$$\varphi_0=2\tan^{-1}\frac{a}{b-\left(c+1\right)} \tag{42}$$

$\theta_i=\pi$ in this situation. The curve gradient at the extreme point cannot be determined. After limit value analysis

under the small change δ, it can be known that the left limit and right limit are:

$$\lim_{\delta \to -0} \frac{d\theta_i}{d\varphi} = \sqrt{1+c} \tag{43}$$

$$\lim_{\delta \to -0} \frac{d\theta_i}{d\varphi} = -\sqrt{1+c} \tag{44}$$

According to above analysis, the relation curve between arm angle and θ_i of cosine type is shown in Fig.4:

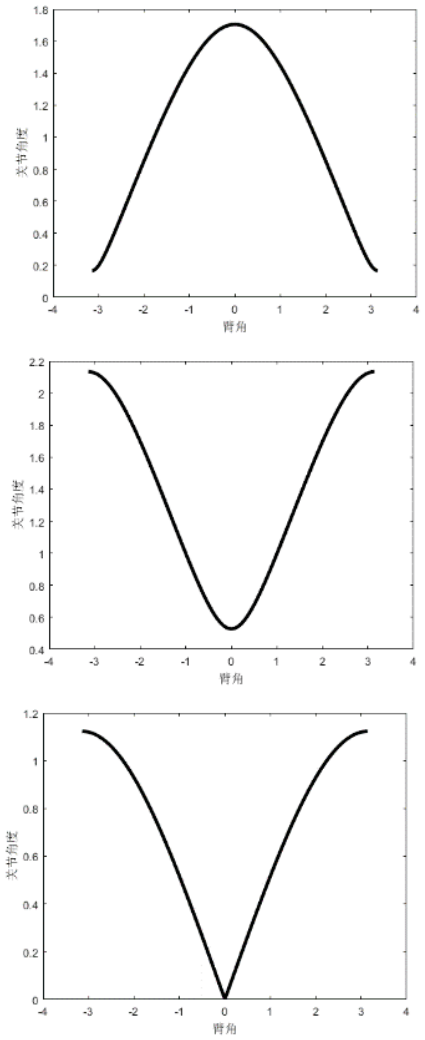

Fig.4 Relation Curve of Cosine Type

C. Selection of Arm Angle Parameters

In the process of designing the robot arm, seven joint axes cannot freely rotate between $[-\pi, \pi]$. The range of each joint is limited:

$$\theta_i^l \le \theta_i \le \theta_i^u \left(i = 1, 2, \cdots, 7\right) \tag{45}$$

θ_i^l and θ_i^u represent the lower limit and the upper limit of θ_i movement range respectively.

It can be known that the relationship between arm angle and inverse kinematics solution is nonlinear and the relation curves between rotation angle and arm angle of different joint axes are in different forms. When each joint axis cannot move freely in fails in $[-\pi, \pi]$, the arm angle is also not in scope $[0, 2\pi]$.

As for the single rotary joint, when the rotation angle θ_i is restricted by θ_i^l and θ_i^u, the scope of valid arm angle is also limited:

$$\psi_i = \bigcup_{j=1}^{n_i} \psi_{ij} \tag{46}$$

Because the valid interval may not be continuous. Thus the valid interval is the union of different groups.

And the valid arm angle for the manipulator must meet the requirement of 7 joints:

$$\psi = \bigcap_{i=1}^{7} \psi_i$$

when ψ is null, the target pose is not reachable.

D. Joint Limit Avoidance

During inverse kinematics, the kinematic solution shall be designed to ensure the result meets the target pose constraint as well as joint limit avoidance, which can maintain the manipulator's ability of performing actions near the target point.

Firstly, from the previous analysis, the calculation of elbow joint rotation angle is unrelated to the arm angle.

Secondly, the shoulder and wrist can be abstracted as spherical joints with three rotational degrees of freedom. R is the actual rotation matrix of the spherical joint and R^d is the desired rotation matrix.

When the actual rotation matrix is approaching the desired rotation. $R\left(R^d\right)^T$ approaches the unit matrix. Supposing ϕ refers to three rotation angles corresponding to $R\left(R^d\right)^T$ matrix, then, ϕ tends to be zero.

As for the shoulder joint, supposing θ_i^d represents the expected joint angle, and R_3^{0d} represents the expected rotation matrix. The deviation between it and the actual matrix can be expressed as:

$$R_3^0\left(R_3^{0d}\right)^T = I_3 + \sin\phi_s\left[u_s^0\times\right] + \left(1-\cos\phi_s\right)\left[u_s^0\times\right]^2 \quad (48)$$

wherein, u_s represents the unit vector of rotation axis and the ϕ_s represents the rotation angle of rotation axis.

And the we have:

$$trace\left(R_3^0\left(R_3^{0d}\right)^T\right) = a_s\sin\varphi_s + b_s\cos\varphi_s + c_s$$
$$= 1 + 2\cos\varphi_s$$

wherein,

$$a_s = trace\left(A_s\left(R_3^{0d}\right)^T\right)$$
$$b_s = trace\left(B_s\left(R_3^{0d}\right)^T\right)$$
$$c_s = trace\left(C_s\left(R_3^{0d}\right)^T\right)$$

Therefore, minimizing the φ_s equals to maximizing the objective function:

$$f_s(\varphi) = a_s\sin\varphi_s + b_s\cos\varphi_s + c_s$$

The above formula has two extreme points:

$$\varphi_s^- = 2\tan^{-1}\frac{-b_s - \sqrt{a_s^2+b_s^2}}{a_s} \quad (49)$$

$$\varphi_s^- = 2\tan^{-1}\frac{-b_s + \sqrt{a_s^2+b_s^2}}{a_s} \quad (50)$$

Analyzing the second derivative of $f_s(\varphi)$, $f_s(\varphi)$ takes maximum or minimum at two extreme points.

Similarly, for the wrist joint, R_7^{4d} represents the expected rotation matrix, and θ_i^d represents the expected joint angle. We have:

$$f_w(\varphi) = a_w\sin\varphi_w + b_w\cos\varphi_w + c_w$$

We can obtain:

$$\varphi_w^- = 2\tan^{-1}\frac{-b_w - \sqrt{a_w^2+b_w^2}}{a_w} \quad (51)$$

$$\varphi_w^- = 2\tan^{-1}\frac{-b_w + \sqrt{a_w^2+b_w^2}}{a_w} \quad (52)$$

are extreme points of $f_w(\varphi)$, respectively.

As for the whole process of inverse kinematics, the global optimal solution can be obtained by combining objective functions as follows:

$$f(\varphi) = \frac{r_s f_s(\varphi) + r_w f_w(\varphi)}{r_s + r_w} \quad (53)$$

Thus, the optimal φ value is one of two angles below:

$$\varphi^- = 2\tan^{-1}\frac{-b - \sqrt{a^2+b^2}}{a^2} \quad (54)$$

$$\varphi^- = 2\tan^{-1}\frac{-b + \sqrt{a^2+b^2}}{a^2} \quad (55)$$

After the optimal arm angle φ is obtained, projecting φ to the valid arm angle interval and choosing optimal arm angle φ^{opt}:

1) $\varphi^{opt} = \varphi$ when the φ is in the ψ;

2) $\varphi^{opt} = \min dist(\varphi,\psi)$ when the φ isn't in the ψ.

IV. Simulation && Verification

Verification and simulation is conducted using the design parameters of AUBO MRA7A redundant manipulator, which is shown in Fig.5.

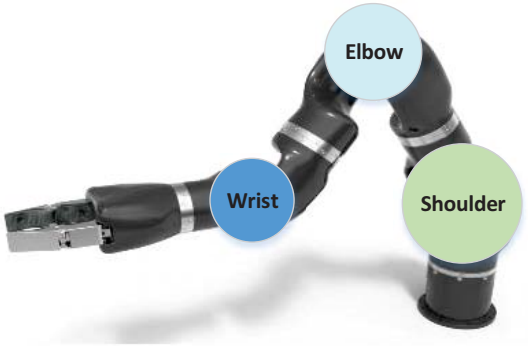

Fig.5 MRA7A Redundant Manipulator

A. Robotics Toolbox Simulation

The robotics toolbox is used to verify the correctness of forward kinematics and inverse kinematics. When the rotation angles are all 0, the manipulator's pose is shown in Fig.6.The manipulator is in an upright position. The red cylinders represent rotational degree of freedom.

The desired joint angle is (0,0,0,0,0,0,0) and the weight in (53) is all 1.

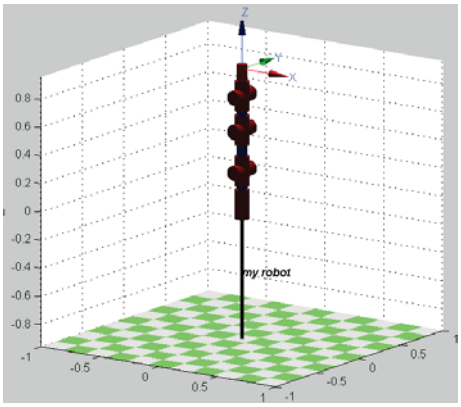

Fig.6 Manipulator When All Rotation Angle is 0

Firstly, the target pose of the end effector is:

$$\tilde{x}_7^0 = \begin{bmatrix} 0.4 & -0.05 & 0.1 \end{bmatrix}^T$$

$$\tilde{R}_7^0 = \begin{bmatrix} -1 & 0 & 0 \\ 0 & 1 & 0 \\ 0 & 0 & -1 \end{bmatrix}$$

The result of inverse kinematics is:

$$\theta = \begin{bmatrix} -0.1347, 0.8057, 0.0175, 1.4162, -0.0159, 0.9198, 0.9198 \end{bmatrix}^T$$

As is shown in Fig.7:

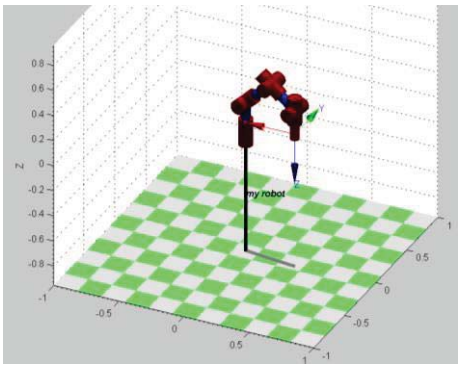

Fig.7 Manipulator Corresponding to Target Pose 1

The arm angle ranges corresponding to the ranges of joint axes are:

$$\psi_1 = \begin{bmatrix} -\pi, \pi \end{bmatrix}$$
$$\psi_2 = \begin{bmatrix} -\pi, \pi \end{bmatrix}$$
$$\psi_3 = \begin{bmatrix} -3.06, 3.06 \end{bmatrix}$$
$$\psi_4 = \begin{bmatrix} -\pi, \pi \end{bmatrix}$$
$$\psi_5 = \begin{bmatrix} -3.0859, 3.0859 \end{bmatrix}$$
$$\psi_6 = \begin{bmatrix} -2.1168, 2.1168 \end{bmatrix}$$
$$\psi_7 = \begin{bmatrix} -\pi, \pi \end{bmatrix}$$

The common interval is: $\psi = \begin{bmatrix} -2.1168, 2.1168 \end{bmatrix}$.

The optimal arm angle under joint limit avoidance constraint is $\varphi = 0.0127$, which is in the common interval. Thus $\varphi^{opt} = \varphi$.

In the other case, the target pose is:

$$\tilde{x}_7^0 = \begin{bmatrix} 0.2 & 0.35 & 0.4 \end{bmatrix}^T$$

$$\tilde{R}_7^0 = \begin{bmatrix} 0 & -1 & 0 \\ 0 & 0 & 1 \\ -1 & 0 & 0 \end{bmatrix}$$

The result of inverse kinematics is:

$$\theta = \begin{bmatrix} -0.1135, 0.1982, 0.6497, 1.9365, -1.2170, -0.8816, 0.0.8710 \end{bmatrix}^T$$

As is shown in Fig.7:

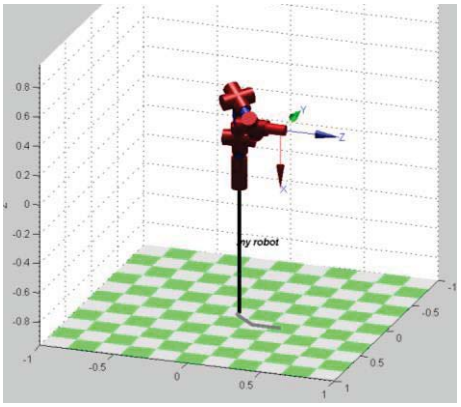

Fig.8 Manipulator Corresponding to Target Pose 2

The arm angle ranges corresponding to the ranges of joint axes are:

$$\psi_1 = \begin{bmatrix} -\pi, \pi \end{bmatrix}$$
$$\psi_2 = \begin{bmatrix} -\pi, \pi \end{bmatrix}$$
$$\psi_3 = \begin{bmatrix} -3.036, 3.036 \end{bmatrix}$$
$$\psi_4 = \begin{bmatrix} -\pi, \pi \end{bmatrix}$$
$$\psi_5 = \begin{bmatrix} -\pi, \pi \end{bmatrix}$$
$$\psi_6 = \begin{bmatrix} -\pi, -2.3892 \end{bmatrix} \cup \begin{bmatrix} -1.5745, \pi \end{bmatrix}$$
$$\psi_7 = \begin{bmatrix} -2.8569, 3.1277 \end{bmatrix}$$

The common interval is obtained is as:

$$\psi = \begin{bmatrix} -2.8569, -2.3892 \end{bmatrix} \cup \begin{bmatrix} -1.5745, 3.0360 \end{bmatrix}$$

The optimal arm angle under joint limit avoidance constraint is $\varphi = 0.1424$, which is in the common interval. Thus $\varphi^{opt} = \varphi$.

Furthermore, the simulation of drawing square in Cartesian space is shown in Fig.9.

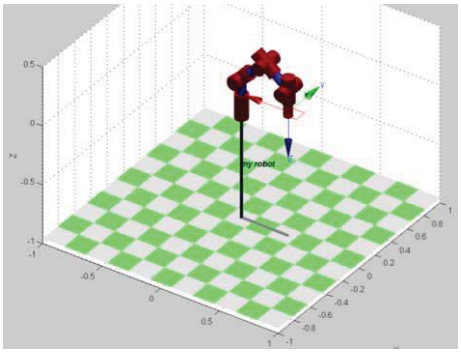

Fig.9 Drawing the Square by End Actuator

B. *Simulation on the ROS platform*

The 3D simulation environment of robot arm is built on the ROS platform, as shown in Fig.10.

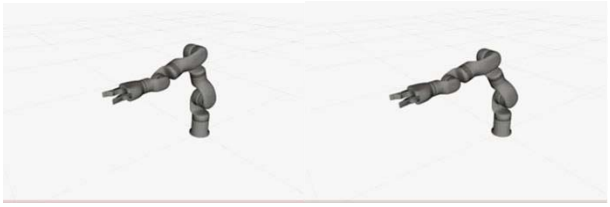

(a) Movement along the X direction

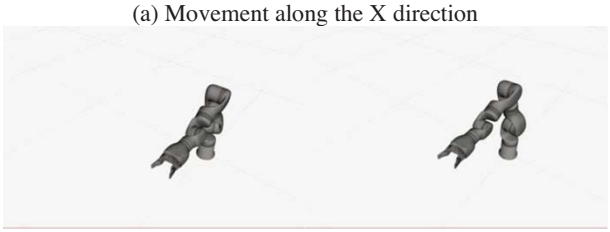

(b) Movement along the Y direction

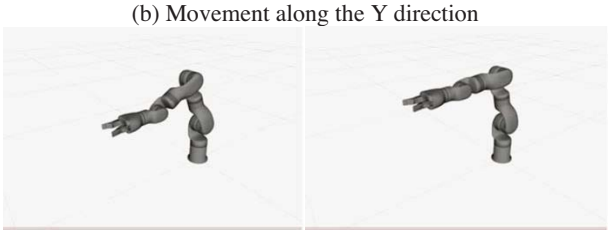

(c) Movement along the Z direction

(d) Rotation along the X direction \

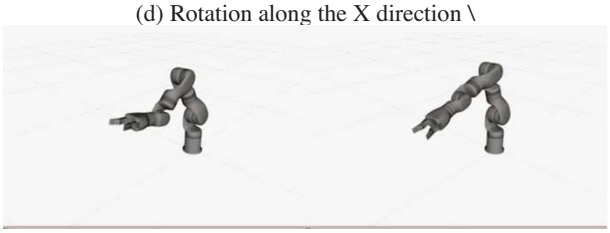

(e) Rotation along the Y direction

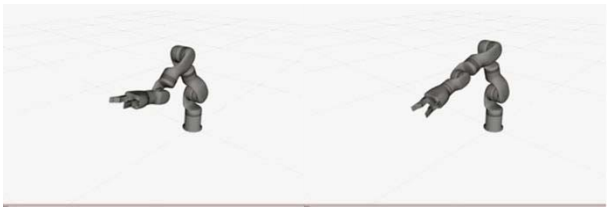

(f) Rotation along the Z direction

Fig.10 Movement of End Actuator in Cartesian Space

With the coordination of 7 rotational joint, the end effector can produce linear motions and rotational motions. As continuous movement is the basis for robot controlling and planning, the proposed method can be integrated to applications easily.

V. CONCLUSIONS

The main meaning of this article is as follows:

1. An analytical inverse kinematics method of redundant manipulator is proposed, which takes the arm angle constraint to realize the decoupling of redundancy. And inverse kinematic derivation and arm angle optimization process is detailed.

2. Compared with the previous literature, this article lists the relationship curve characteristics in detail, providing reliable guidance for engineering development and deployment;

3. Transform the joint limit avoidance constraints to quantified optimization problem and derive an analytical relationship between arm angle and constraints, which can improve the movement ability of manipulator for applications in successive manner.

4. From abstract model to actual application, the method proposed is verified by robotics toolbox and ROS platform respectively which confirms correctness and reliability of the method.

In the subsequent work, application and development of redundant manipulator in space application will be conducted based on the proposed algorithm.

ACKNOWLEDGMENT

This work was supported by the Verification and Application Project of Core Electronic Devices in Missile Control System under Grant No.2017ZX01013101-002.

REFERENCES

[1] BoumansR , Heemskerk C . The European Robotic Arm for the International Space Station[J]. Robotics and Autonomous Systems, 1998, 23(1-2):17-27.

[2] Reed B B , Smith R C , Naasz B J , et al. The Restore-L Servicing Mission[C]// Aiaa Space.

[3] Lee S ,Bejczy A K . Redundant arm kinematic control based on parameterization[C]// Robotics and Automation, 1991. Proceedings. 1991 IEEE International Conference on. IEEE, 1991: 458-465.

[4] Zhang Y , Chen S , Li S , et al. Adaptive Projection Neural Network for Kinematic Control of Redundant Manipulators With Unknown

Physical Parameters[J]. IEEE Transactions on Industrial Electronics, 2017:1-1.

[5] Toshani H , Farrokhi M . Real-time inverse kinematics of redundant manipulators using neural networks and quadratic programming: A Lyapunov-based approach[J]. Robotics & Autonomous Systems, 2014, 62(6):766-781.

[6] Yoshikawa T . Manipulability and redundancy control of robotic mechanisms[C]// Proceedings. 1985 IEEE International Conference on Robotics and Automation. IEEE, 2003: 3239-3243.

[7] Ki Suh, Hollerbach, J.M. Local versus global torque optimization of redundant manipulators[C]// IEEE International Conference on Robotics & Automation. IEEE, 1987: 619–624.

[8] Colbaugh R , Seraji H , Glass K L . Obstacle avoidance for redundant robots using configuration control[J]. Journal of Field Robotics, 1989, 6(6):721-744.

[9] Nakamura Y , Hanafusa H , Yoshikawa T . Task-Priority Based Redundancy Control of Robot Manipulators[J]. International Journal of Robotics Research, 1987, 6(2):3-15.

[10] Yan L , Mu Z , Xu W . Analytical inverse kinematics of a class of redundant manipulator based on dual arm-angle parameterization[C]// Conference -ieee International Conference on Systems. IEEE, 2014:3744-3749.

[11] Nenchev, Dragomir N, Tsumaki, Yuichi, Takahashi, Mitsugu. Singularity-consistent kinematic redundancy resolution for the S-R-S manipulator[C]// IEEE/RSJ International Conference on Intelligent Robots & Systems. IEEE, 2004: 3607-3612.

[12] M. Hollerbach, Optimum kinematic design for a seven degree of freedom manipulator, Tech. rep., MIT Artificial Intellegence Laboratory, Cambridge (1985).

[13] Chen Y , Chen Y , Guo J . An optimization algorithm to expand the reduced workspace with fixed-joint method for redundant manipulator[C]// IEEE Workshop on Advanced Robotics & Its Social Impacts. IEEE, 2016.

[14] Shimizu M , Yoon W K , Kitagaki K . A Practical Redundancy Resolution for 7 DOF Redundant Manipulators with Joint Limits[C]// Robotics and Automation, 2007 IEEE International Conference on. IEEE, 2007.

[15] Shimizu, M., Kakuya, H., Yoon, W. K. (2008). Analytical inverse kinematic computation for 7-DOF redundant manipulators with joint limits and its application to redundancy resolution. IEEE Transactions on Robotics, 24(5), 1131-1142.

[16] Practical analytical inverse kinematic approach for 7-DOF space manipulators with joint and attitude limits[J]. Intelligent Service Robotics, 2015, 8(4):215-224.

[17] Yu C , Jin M , Liu H . An analytical solution for inverse kinematic of 7-DOF redundant manipulators with offset-wrist[C]// Mechatronics and Automation (ICMA), 2012 International Conference on. IEEE, 2012.

[18] Singh, G. K., &Claassens, J. An analytical solution for the inverse kinematics of a redundant 7dof manipulator with link offsets. In 2010 IEEE/RSJ International Conference on Intelligent Robots and Systems (pp. 2976-2982). IEEE.

[19] Faria C , Ferreira F , Erlhagen W , et al. Position-based kinematics for 7-DoF serial manipulators with global configuration control, joint limit and singularity avoidance[J]. Mechanism & Machine Theory, 2018, 121:317-334.

[20] T. Asfour and R. Dillmann, “Human-like motion of a humanoid robot arm based on a closed-form solution of the inverse kinematics problem,” in Proc. 2003 IEEE/RSJ Int. Conf. Intell. Robots Syst., pp. 1407–1412.

[21] Y. Taki and K. Sugimoto, “Classification of singular configurations for 7-DOF manipulators with kinematic redundancy,” in Proc. 6th Jpn–Fr. 4th Asia–Eur. Mechatronics Congr., 2003, pp. 438–443.